Genotype-phenotype discrepancy among family members carrying a novel glucokinase mutation: insights into the interplay of GCK-MODY and insulin resistance

Shuhui Ji[1,#], Hua Shu[1,#], Hongqiang Zhao[2,3,#], Yuanyuan Ye[1], Xuan Liu[1], Shanshan Chen[1], Ying Yang[1], Wenli Feng[1], Jingting Qiao[1], Jinyang Zhen[1], Xiong Yang[2,3], Ziyue Zhang[1], Yu Fan[1], Yadi Huang[1], Qing He[1], Minxian Wang[2,3,4,5,6,7,‡], Kunlin Wang[1,‡], Ming Liu[1,‡]

[1] Department of Endocrinology and Metabolism, Tianjin Medical University General Hospital, Tianjin, 300052, China

[2] National Genomics Data Center, China National Center for Bioinformation, Beijing, China

[3]Beijing Institute of Genomics, Chinese Academy of Sciences, Beijing, China

[4]College of Future Technology, Sino-Danish College, University of Chinese Academy of Sciences, Beijing, 100049, China.

[5]Department of Cardiovascular Surgery, Zhongnan Hospital of Wuhan University, Wuhan 430071, China

[6]Hubei Provincial Engineering Research Center of Minimally Invasive Cardiovascular

19 Surgery, Wuhan 430071, China

20 [7]Wuhan Clinical Research Center for Minimally Invasive Treatment of Structural

21 Heart Disease, Wuhan 430071, China

22 [#]Authors contribute equally to the work.

23 [‡]To whom correspondence may be addressed. Ming Liu, Department of

24 Endocrinology and Metabolism, Tianjin Medical University General Hospital, #154

25 Anshan Road, Heping District, Tianjin, 300052, China. Email: mingliu@tmu.edu.cn;

26 Kunling Wang, email: zp-sd@126.com; Minxian Wang, email: wangmx@big.ac.cn

27

28

29

30

31

32

33

34

35

36

Abstract

Aims/Hypothesis: Heterozygous inactivating mutations in the glucokinase (GCK) gene are known to cause maturity-onset diabetes of the young (GCK-MODY). We identified a novel variant of uncertain significance (VUS) GCK mutation (c.77A>T, p.Q26L) in two family members presenting markedly different severities of diabetic phenotypes. This study aimed to elucidate the potential diabetogenic effect of GCK-Q26L and to explore the mono- and poly-genetic background attributing to different diabetes phenotypes.

Methods: Whole-exome sequencing (WES) and genetic analyses, including polygenic risk score (PRS) assessments, were performed in three members of a family with early-onset diabetes. To elucidate the impact of the GCK-Q26L mutation on glucose homeostasis, a global knock-in mouse model harboring this mutation in both heterozygous and homozygous states was generated. Insulin content and insulin secretion response to glucose and potassium were evaluated in isolated islets. Furthermore, the effects of dorzagliatin (a glucokinase activator, GKA) and liraglutide (a glucagon like peptide 1 receptor agonist, GLP-1RA) on glucose tolerance and insulin secretion were assessed in GCK-Q26L mutant mice.

Results: The proband, who inherited the GCK-Q26L mutation from her father (presenting with non-progressive, mildly elevated blood glucose), exhibited severe diabetic phenotypes including polydipsia, polyuria, polyphagia, weight loss, and

ketosis, accompanied by significant dyslipidemia. Genetic analyses revealed that the proband's severe phenotypes and metabolic profiles were associated with a high polygenic risk score (PRS) for insulin resistance that was inherited from her mother. Global heterozygous GCK-Q26L knock-in mice showed a mild increased fasting blood glucose, impaired glucose tolerance (IGT), and decreased serum insulin. Homozygous GCK-Q26L mice presented more severe phenotypes compared to their heterozygous counterparts, confirming the diabetogenic nature of the GCK-Q26L mutation. Further analyses indicated that GCK-Q26L did not affect insulin sensitivity and islet insulin content. However, GCK-Q26L blunted islet responsiveness to different glucose concentrations and markedly impaired glucose-stimulated insulin secretion (GSIS) without affecting potassium chloride-stimulated insulin secretion (KSIS) and glucose inhibitory effects on glucagon secretion. Both GKA and GLP-1RA enhanced insulin secretion and improved glucose tolerance in mutant mice.

Conclusions/Interpretation: This study demonstrates that GCK-Q26L is a GCK-MODY causing mutation. The interplay of GCK-Q26L with a high PRS for insulin resistance contributes to severe diabetic phenotypes. The findings not only expend the list of GCK-MODY causing mutations originally classified as VUS mutations, but also provides insights into interactions of GCK-MODY with polygenic risks of type 2 diabetes, highlighting the importance of considering polygenic backgrounds in the assessment and management of monogenic diabetes.

Keywords: monogenic diabetes, glucokinase, GCK-MODY, insulin resistance, polygenic risk score (PRS)

Research in Context

What is already known about this subject?

Heterozygous inactivating mutations in the GCK gene cause GCK-MODY, an autosomal dominant disorder characterized by mild hyperglycemia present from birth.

Insulin resistance can be influenced by multiple genetic polymorphisms, contributing to varying diabetes phenotypes.

What is the key question?

Is the newly discovered GCK mutation pathogenic?

Do the interactions between the GCK mutation and PRS for insulin resistance influence the phenotypic variability in patients carrying GCK-MODY?

What are the new findings?

The study demonstrates GCK-Q26L impairs GSIS and causes diabetes, establishing it as a novel GCK-MODY causing mutation originally classified as a VUS mutation.

The GCK-Q26L knock-in mouse line replicates phenotypes of GCK-MODY in humans, establishing it as an excellent model for GCK-MODY.

The phenotypic variability in patients with GCK-MODY can be significantly influenced by high-risk genetic predisposition of type 2 diabetes.

Both GKA and GLP-1RA enhance insulin secretion and improve glucose tolerance in GCK-Q26L mutant mice, suggesting that they are favorite options for treatment of patients with GCK-MODY and insulin resistance.

How might this impact clinical practice in the foreseeable future?

Recognizing atypical presentations of monogenic diabetes influenced by polygenic factors can enhance diagnostic accuracy and personalized management.

Genetic testing and polygenic risk score assessments can help identify patients at higher risk of severe phenotypes, allowing for earlier and more targeted interventions.

Background

Glucokinase (GCK), a key enzyme in the glycolytic pathway, plays a critical role in glucose metabolism. It acts as a glucose sensor in pancreatic β cells and regulates insulin secretion in response to blood glucose levels [1, 2]. The unique kinetic properties of GCK make it ideal for this regulatory role, as it responds to even small changes in glucose concentration within the physiological range [2, 3]. Heterozygous inactivation mutations of GCK are known to cause maturity-onset diabetes of the young type 2 (MODY 2, also known as GCK-MODY), an autosomal dominant form

114 of diabetes. These GCK inactivation mutations impair enzymatic activity, affecting
115 glucose sensing of pancreatic β cells, resulting in a higher set point for insulin
116 secretion, and therefore leading to mild and non-progressive elevated fasting blood
117 glucose (FBG) from an early age [4, 5]. Notably, unlike other types of diabetes, GCK-
118 MODY does not typically increase the risks of chronic micro- and macrovascular
119 complications of diabetes [6]. Therefore, the current recommendations for the
120 management of GCK-MODY emphasize lifestyle management and regular blood
121 glucose monitoring rather than active treatment with hypoglycemic agents [6, 7].
122 However, the clinical presentation of GCK-MODY can vary significantly among
123 individuals, even within the same family. The underlying mechanisms for this
124 variability remain incompletely understood.

125 Insulin resistance associated with multiple genetic and environmental factors is a key
126 feature of type 2 diabetes (T2D) [8]. Recent studies have identified various genetic
127 polymorphisms contributing to insulin resistance, each adding a small risk but
128 cumulatively having a significant impact [9]. A high polygenic risk score (PRS) for
129 insulin resistance aggregates the effect of numerous risk alleles, increasing the
130 likelihood of T2D development [10, 11]. Additionally, a high PRS for T2D may also
131 interact with monogenic diabetes causing mutations, leading to atypical and severe
132 diabetic phenotypes that challenge the traditional approaches for classification and
133 management of different types of diabetes [8, 12-14]. Understanding the interaction
134 between these genetic factors is crucial for developing personalized treatment

135 strategies [15].

136 In this study, we identified a novel variant of uncertain significance (VUS) GCK
137 mutation (c.77A>T, p.Q26L) in two members of a family exhibiting markedly
138 different severities of diabetic phenotypes. A global knock-in mouse model
139 established that GCK-Q26L impaired insulin secretion of β cells response to glucose
140 and caused an increase of FBG and an impairment of glucose tolerance, thereby
141 confirming this mutation is a GCK-MODY causing mutation. Genetic analyses
142 revealed the interplay between the GCK-MODY mutation and a high PRS for insulin
143 resistance contributed to the severe diabetic phenotypes in the proband carrying GCK-
144 Q26L. The study not only expends the list of GCK-MODY causing mutations
145 originally classified as VUS mutations, but also highlights genetic bases underlying
146 phenotype heterogeneities of patients with monogenic diabetes.

147

148 ## Materials and Methods

149 **Patients.** The clinical information of the proband and her family members was
150 detailed in Table 1, collected and documented in Tianjin Medical University General
151 Hospital. Informed consent was obtained from all family members. The study was
152 approved by the Tianjin Medical University General Hospital Ethics Committee
153 (IRB2017-047-01).

154 **Genetic Testing and Analyses.** DNA was extracted from proband's white blood cells

155 for targeted gene capture, followed by whole-exome sequencing (WES) utilizing
156 massive parallel next-generation sequencing (NGS). The identified GCK gene
157 mutation was further confirmed by Sanger sequencing, the primers for the forward-
158 and reverse-strand were 5'-TGTGGGGGAGATGCCCCG-3' and 5'-
159 ACCAGAGGAGCCAAGGGTGAG-3', respectively. Members of the proband's
160 family (father, mother and grandfather) were recruited and checked for the mutation
161 using Sanger sequencing. Furthermore, the family members (father and mother) also
162 underwent WES sequencing.

163 **Definitions for Insulin Resistance.** Insulin resistance (IR) was measured as the ratio
164 of triglycerides (TG) to high-density lipoprotein cholesterol (HDL-C) as described
165 elsewhere [9, 16-19] (ESM Fig. 4). To correct the potential effect of cholesterol
166 lowering medications, we adjusted the levels of TG and HDL-C before calculating IR
167 with detailed adjustment in ESM Table 4.

168 **Genotype quality control and imputation.** The proband trios were genotyped by
169 Affymetrix Axiom whole-genome Asian Screening Array (ASA Array) with calling
170 rate > 99%. Kingship (ESM Table1) and sex (ESM Table2) were further validated
171 with genetically inferred ones. The data was merged with non-close related samples
172 from the 1000 Genomes Project with ambiguous variants (A/T or G/C alleles)
173 removed. This was followed by a series of quality controls in samples with a
174 missingness rate > 5%, or heterozygosity out of 5 standard deviations were excluded,

175 and variants with a missing rate > 1% or Hardy-Weinberg equilibrium with a P-value
176 < 1 × 10^−6 were excluded. Then, principal component analysis (PCA) was
177 conducted, and ancestry was inferred by the PCA clusters. Finally, the genotype was
178 further imputed on the TOPMed imputation server [20] (ESM Fig. 3), and variants
179 with imputation quality score (INFO) < 0.8 were removed in subsequent analysis.

180 **PRS assessment.** We directly utilized the polygenic scores model for insulin
181 resistance developed by Lotta et al.[8] from the PGS Catalog and calculated the PRS
182 for our datasets together with 1000 Genomes Project East Asian samples by PLINK
183 2.0 [21]. To confirm the association between PRS and IR, we also calculated the PRS
184 for the samples (424,068 passed quality control) from the UK Biobank (ESM Table 3)
185 under application number 89885, following the same procedures. The PRS was
186 further corrected by the value of principal components (PCs) for potential population
187 structure and batch effects and standardized to normal distribution for further
188 statistical analysis.

189 **Mice.** We commissioned GemPharmatech Co., Ltd. to create a global knock-in GCK-
190 Q26L mouse model. The Q26L site-directed mutagenesis was introduced in exon 2 of
191 mouse GCK-201, changing the codon for the 26th amino acid from CAG to CTG and
192 inserting MYC before the stop codon (ESM. Fig.1a). All mice were bred on a
193 C57BL/6J background and housed in temperature (22–25 °C) and humidity (55 ± 5%)
194 controlled rooms with a 12-hour light/dark cycle. All animal experimental protocols

195 were approved by the Internal Animal Welfare Committee at Chu Hsien-I Memorial
196 Hospital (Metabolic Diseases Hospital) of Tianjin Medical University.

197 **Glucose and insulin tolerance.** Mice were fasted for 6 hours before intraperitoneal
198 glucose tolerance tests (IPGTT). Glucose was administered via intraperitoneal
199 injection at 2 g/kg body weight. Blood glucose was measured from the tail vein at 0,
200 15, 30, 60, and 120 minutes using an automated glucose meter (Roche, ACCU-CHEK,
201 Germany). ELISA kits were used to measure plasma insulin (EZassay, China), and
202 glucagon (Ruixin, China). For the intraperitoneal insulin tolerance test (IPITT), after a
203 4-hour fast, mice received an intraperitoneal injection of 0.7 U/kg body weight of
204 insulin (Aspart, Novo Nordisk A/S, Denmark). Dorzagliatin (Desano, China) and
205 Liraglutide (Solarbio, China) were administered to mice by gavage or intraperitoneal
206 injection, respectively, 90 minutes before the start of the IPGTT.

207 **Measurement of insulin and glucagon secretion.** Islet isolation, glucose-stimulated
208 insulin secretion (GSIS), and potassium-stimulated insulin secretion (KSIS) were
209 performed as previously described [22], glucose-inhibited glucagon secretion was
210 performed simultaneously with GSIS. For the dose-dependent effects of glucose on
211 insulin secretion, isolated pancreatic islets were sequentially cultured in Krebs-Ringer
212 bicarbonate HEPES (KRBH) buffer with glucose concentrations of 2.8 mM, 3.3 mM,
213 4.5 mM, 5.6 mM, and 7 mM for 2 hours each. After incubation, supernatants were
214 collected, and the islets were homogenized. Secreted insulin and islet insulin content

215 were measured using ELISA kits (EZassay, China). The secretion efficiency was
216 calculated with secreted insulin in the media normalized to islet insulin content.

217 **Islet perfusion assays.** Islet perfusion assays were performed as previously described
218 [22]. The liquid input flow rate was 150 μl/min, with samples collected every minute.
219 Insulin secretion at each time point was quantified using the Wide Range Insulin
220 Assay Kit (EZassay, China) according to the manufacturer's instructions.

221 **Western blot analysis.** Equal amounts of islet proteins were loaded onto 4-12%
222 NuPage gradient gels (Thermo, USA), while other tissues were loaded onto 12.5%
223 gels (US EVERBRIGHT, China). The antibodies used in this study were as follows:
224 anti-GCK (Cat: A00884-1, BOSTER, China), anti-c-MYC (Cat: RMYC-45A-2, ICL,
225 USA), anti-GAPDH (Cat: AC033, Abclonal, China), anti-insulin (homemade).

226 **Immunofluorescence**. Mouse pancreas was fixed, sectioned, and stained with
227 different primary antibodies followed by Alexa-Fluor-conjugated secondary
228 antibodies. The antibodies used in this study were as follows: anti-insulin
229 (homemade), anti-glucagon (Cat: G2654, Sigma, USA), anti-somatostatin (Cat:
230 ab30788, abcam, USA). Fluorescent images were visualized using an Axio Imager
231 M2 microscope (Carl Zeiss, Germany).

232 **Statistics.** All experiments were performed independently at least three times. Data
233 are presented as means ± SEM. Statistical analyses were conducted using GraphPad
234 Prism 8 software. An unpaired Student's t-test was used for data analysis, with a

threshold of $P < 0.05$ to declare statistical significance.

Results

Identification of a novel variant of uncertain significance (VUS) GCK mutation in a family with early onset diabetes. In the clinic, we observed a special case of diabetes. The female proband was diagnosed with diabetes at age teens, presenting with polydipsia, polyuria, polyphagia, weight loss, and ketosis. Her body mass index (BMI) was 22.66 kg/m², and islet autoantibodies were all negative. Initial FBG was 6–7 mmol/L, 2hBG was 15–18 mmol/L, and HbA1c was 113.12 mmol/mol (12.5%). The result of the 75g oral glucose tolerance test (OGTT) confirmed the diagnosis of diabetes and indicated the presence of insulin resistance and inadequate insulin secretion in response to glucose load. (Fig. 1a). She was treated with Metformin (0.5 g TID) and Insulin glargine (18 U QN), with occasional monitoring showing FBG of 5–7 mmol/L and 2hBG of 13–14 mmol/L. She continued this treatment inconsistently, without dietary control, regular exercise, or routine SMBG. After 2.5 years, she discontinued insulin and continued Metformin (0.5 g TID), with occasional FBG readings of 6–7 mmol/L. Five years post-diagnosis, her FBG increased to 7.5–13.2 mmol/L, HbA1c to 132.79 mmol/mol (14.3%), and BMI to 26.76 kg/m². Her regimen was changed to Metformin (0.5 g TID), Insulin aspart (8-6-6 U before meals), and Insulin glargine (12–16 U QN), but glycemic control remained poor, with FBG of 7–

255 10 mmol/L. Her father was diagnosed with diabetes at thirties, treated with Metformin
256 0.5 g BID and Vildagliptin 50 mg BID, with FBG of 5–7 mmol/L. Seven years later,
257 his regimen was changed to Metformin 0.5 g TID and occasional Dapagliflozin,
258 maintaining FBG at 6.5 mmol/L and HbA1c at 60.66 mmol/mol (7.7%). Her
259 grandfather was diagnosed with diabetes at fifties, managed with oral hypoglycemic
260 agents. Her mother was found to have pre-diabetes at forties based on blood glucose
261 and HbA1c levels. Clinical details of the proband and her family were summarized in
262 Table 1.

263 Given the proband's negative islet autoantibodies and family history, we suspected
264 monogenic diabetes and performed genetic screening. DNA sequencing revealed a
265 novel heterozygous missense mutation, c.77A>T, in exon 2 of the GCK gene,
266 resulting in a glutamine-to-leucine substitution at position 26 (p.Q26L), which had not
267 been reported yet. According to American College of Medical Genetics and Genomics
268 (ACMG) and the Association for Molecular Pathology (AMP) in 2015 guidelines, the
269 mutation was classified as a variant of uncertain significance (VUS) with evidence
270 PM1+PM2+PP2. The biological information analysis software SIFT
271 (http://provean.jcvi.org/index.php) predicts that the heterozygous variation c.77A>T
272 (p.Q26L) in the GCK gene is deleterious. PolyPhen2 (http://genetics.bwh.harvard.edu)
273 predicts a score of 0.026, indicating that the GCK gene mutation c.77A>T (p.Q26L) is
274 benign. Additionally, the frequency of this mutation in the general (normoglycemic)
275 population according to gnomAD (v4.1.0) is 0. Pedigree analysis showed that the

276 proband's father had the same heterozygous mutation, while the grandfather and
277 mother did not (Fig. 1b, c).

278 Based on these findings, the proband's diabetes type and the role of the GCK-Q26L
279 mutation in her complex diabetic phenotype remain unclear. However, the father's
280 glycemic profile aligned with typical GCK-MODY characteristics. Therefore, further
281 experiments were conducted to assess the impact of the GCK mutation on protein
282 function.

283

284 **GCK-Q26L is a GCK-MODY causing mutation.** Since GCK-Q26L was classified
285 as a VUS and the proband presented atypical clinical features of GCK-MODY, it
286 remained to be determined whether GCK-Q26L is a diabetes causing mutation. We
287 therefore established a global knock-in mouse model expressing MYC-tagged GCK-
288 Q26L (ESM Fig. 1a). Western blot confirmed the specific expression of MYC-tagged
289 mutant GCK in the liver and islets in a dose-dependent manner in GCK-Q26L
290 heterozygous (Het) and homozygous (Hom) mice (ESM Fig. 1b). We had monitored
291 body weight (BW) and FBG of mutant and wild-type (WT) male mice for 16 weeks.
292 Although the GCK-Q26L mutation did not affect BW, it caused mild, non-progressive
293 elevation of FBG in Het mice, with further elevation observed in Hom mice (Fig. 2a,
294 b). To investigate whether abnormal circulating levels of insulin or glucagon were
295 associated with elevated FBG, we examined fasting serum insulin and glucagon levels.

296 Our findings showed that although glucagon levels were unaffected, serum insulin
297 levels were decreased in 16-week-old mutant mice (Fig. 2c, d). We therefore
298 performed intraperitoneal glucose tolerance test (IPGTT) and found that Het and Hom
299 mice exhibited significantly impaired glucose tolerance and lower serum insulin
300 levels compared to that of WT mice at 3 weeks of age (Fig. 2e, f). The severities of
301 decreased serum insulin and impaired glucose tolerance did not further worsen in 16-
302 week-old mutant mice (Fig. 2g, h). The phenotype of female mice was similar to that
303 of male mice but less severe (ESM Fig. 2). These data established that GCK-Q26L
304 caused non-progressive mild hyperglycemia representing one of classic clinical
305 features of GCK-MODY, confirming that GCK-Q26L is a GCK-MODY mutation.

306

307 **GCK-Q26L does not affect insulin sensitivity and islet insulin content.** Since GCK
308 is also expressed in hepatocytes, we asked whether GCK-Q26L affected insulin
309 sensitivity. We performed intraperitoneal insulin tolerance test (IPITT) and found that
310 GCK mutant did not affect insulin sensitivity (Fig. 3a, b), suggesting that
311 hyperglycemia was mainly due to decreased circulating insulin. To investigate
312 whether reduced serum insulin in Het and Hom male mice is caused by decreased to
313 islet insulin content or insulin secretion, we measured insulin content by two
314 independent approaches (western blots and insulin enzyme-linked immunosorbent
315 assays, ELISA). Both methods consistently showed no substantial differences in

316 insulin content in islets of Het and Hom mice compared to WT mice (Fig. 3c-f). The
317 ratio of proinsulin-to-insulin was also not affected (Fig. 3f). Immunofluorescence
318 analysis revealed no impact of the mutation on the abundance and intraislet
319 composition of insulin-positive, glucagon-positive, and somatostatin-positive cells
320 among three groups (Fig. 3h). Furthermore, western blot results showed no significant
321 differences in endogenous GCK protein expression in the islets among the three
322 groups, indicating that the GCK-Q26L did not affect protein levels of endogenous
323 GCK (Fig. 3d, g).

324

325 **GCK-Q26L impairs glucose-stimulated insulin secretion without affecting**
326 **potassium-stimulated insulin secretion and glucose-inhibited glucagon secretion.**
327 Since the GCK-Q26L caused a decrease of circulating insulin without affecting islet
328 insulin content (Fig. 2-3), we next asked whether it impair insulin secretion. Insulin
329 secretion was monitored in isolated islets exposed to different glucose concentrations
330 (2.8 mM, 3.3 mM, 4.5 mM, 5.6 mM, 7 mM). We found that the curve of glucose
331 concentration-dependent insulin secretion was shifted to right in Het mice (Fig. 4a),
332 suggesting that the glucose threshold for insulin secretion was increased in GCK-
333 Q26L mice. In addition, insulin secretion response to even higher glucose (16.7 mM)
334 was also impaired in Het islets and the response was further diminished in Hom islets
335 (Fig. 4b). Islet perfusion tests with different glucose concentrations further supported

336 these observations (Fig. 4c). However, despite defects in response to glucose, GCK-
337 Q26L did not affect insulin secretion response to potassium in both tests of potassium
338 chloride-stimulated insulin secretion (KSIS) and islet perfusion (Fig. 4d, e).
339 Furthermore, no differences were observed in glucose-inhibited glucagon secretion
340 (GIGS) in Het and Hom mutant mice (Fig. 4f). These data demonstrated that GCK-
341 Q26L impaired the function of GCK as a glucose sensor in β cells, impeding GSIS
342 without affecting KSIS and GIGS.

343

344 **Dorzagliatin restores the glucose threshold for insulin secretion and ameliorates**
345 **glucose tolerance in GCK-Q26L mice.** Dorzagliatin, a novel allosteric glucokinase
346 activator (GKA), improved glycaemic control and was approved in China for the
347 treatment of adult patients with type 2 diabetes [23, 24]. To evaluate the effects of
348 dorzagliatin on insulin secretion and glucose tolerance in GCK-Q26L mice, we firstly
349 treated mice with oral administrations of dorzagliatin, measured fasting blood glucose
350 and insulin levels 90 minutes after treatment, and then performed IPGTT. We found
351 that dorzagliatin significantly decreased FBG and increased fasting insulin levels in
352 both WT, Het, and Hom mutant mice (Fig. 5a, b). IPGTT results further confirmed
353 improvement of glucose tolerance in mutant mice treated with dorzagliatin (Fig. 5c).
354 We further analyzed insulin secretion response glucose and found that dorzagliatin
355 restored the glucose threshold for insulin secretion (Fig. 5d) and improved GSIS (Fig.

356 5e) in GCK-Q26L mutant islets.

357

358 **Liraglutide amplifies insulin secretion response to glucose and ameliorates**
359 **glucose tolerance in GCK-Q26L mice.** Since liraglutide, a glucagon-like peptide-1
360 receptor agonist (GLP-1RA), has an effect of glucose-dependent stimulated insulin
361 secretion, we next asked whether liraglutide could show beneficial effects on insulin
362 secretion and glucose tolerance in GCK-Q26L mice. We conducted similar
363 experiments as dorzagliatin treatment shown in Fig. 5. We found that unlike
364 dorzagliatin, liraglutide did not significantly stimulate insulin secretion in the fasting
365 state both in WT and mutant mice, and only moderately decreased FBG in GCK
366 mutant mice compared with dorazgliatin (Fig. 6a, b). However, liraglutide indeed
367 markedly stimulated insulin secretion and decreased blood glucose 15 minutes after
368 glucose load (Fig. 6c, d), ameliorating overall glucose tolerance (Fig. 6e). In vitro
369 experiments using isolated islets further confirmed that liraglutide improved GSIS
370 (Fig. 6f) and amplified insulin secreation in 5.6 mmol/L glucose (Fig. 6g) in islets
371 from GCK-Q26L mice. Altogether, these results suggest that while both dorzagliatin
372 and liraglutide improve glucose homeostasis, they do so through distinct mechanisms.
373 Dorzagliatin directly enhances the glucose-sensing capability of glucokinase, whereas
374 liraglutide amplifies insulin secretion in response to glucose.

375

376 **A high PRS for insulin resistance is associated with atypical and more severe**
377 **diabetic phenotypes in proband.** The experimental evidence above demonstrates
378 that GCK-Q26L is a GCK-MODY causing mutation. However, although the proband
379 inherited the mutation from her father who presented typical clinical features of GCK-
380 MODY, the proband presented more severe hyperglycemia that did not resemble a
381 classic GCK-MODY (Fig. 1 and Table 1), suggesting that additional factors may
382 contribute to phenotypes of the proband. Indeed, as the disease progressed , the
383 proband became overweight (BMI 26.76 kg/m^2) and developed dyslipidemia with a
384 high Triglyceride (TG) to HDL-cholesterol (HDL-c) ratio, conditions often associated
385 with insulin resistance [19]. Utilizing data from 424,068 individuals in the UK
386 Biobank (UKB), we examined the association between the TG/HDL-c ratio, a
387 surrogate measure of insulin resistance [9, 16-19], with insulin resistance polygenic
388 scores. Results indicated the PRS was significantly associated with the observed
389 TG/HDL-c ratio, that higher PRS levels corresponded with increases in the TG/HDL-
390 c ratio, supporting the relevance of PRS in assessing insulin resistance genetic risk in
391 the population (Fig. 7a). To explore the genetic predisposition of insulin resistance in
392 this family, we conducted a PRS analysis and used the East Asian samples from the
393 1000 Genomes Project samples for evaluate the PRS risk and adjusted for potential
394 population structure confounding through principal component analysis (PCA) (ESM
395 Fig. 5a, b). The PRS analysis of the family indicated the proband inherited a high
396 insulin resistance genetic risk from her mother, who has an IR PRS score ranked in

397 the top 2% in the study population (Fig. 7b). According to previous studies,
398 monogenic risk and polygenic scores may jointly influence the risk of disease [14].
399 These data suggest that the probands' atypical and severe diabetic phenotypes were
400 associated with high PRS for insulin resistance in addition to GCK mutation.

401

402 **Discussion**

403 The identification of the novel GCK-Q26L mutation, originally classified as VUS, in
404 two members of a family with marked differences in PRS for insulin resistance and
405 different severities of diabetes adds to the growing complexities of genetic
406 contributions to the development and progression of diabetes. With multiple
407 independent approaches, we demonstrated that GCK-Q26L did not affect insulin
408 biosynthesis and islet insulin content, but impeded glucose sensing of pancreatic β
409 cells, increasing the threshold of glucose concentration for insulin secretion, impairing
410 GSIS, and therefore causing mild elevated FBG and glucose intolerance. These data
411 established that GCK-Q26L is indeed a pathogenic mutation causing GCK-MODY.

412

413 GCK-MODY typically presents with mild hyperglycemia that is often managed
414 without pharmacological intervention due to low risks of diabetes related chronic
415 complications and the limited efficacy of traditional glucose-lowering medications [4,
416 6]. However, the presence of insulin resistance can complicate the clinical picture,

417 leading to more severe hyperglycemia and necessitating therapeutic intervention. The
418 results from our GCK-Q26L mouse model highlight the potential therapeutic benefits
419 of using GKA and GLP-1RAs in managing diabetes phenotypes influenced by both
420 GCK mutations and polygenic risk factors for insulin resistance. Dorzagliatin is a new
421 a dual-acting GKA that enhances glucokinase activity by binding to its allosteric site,
422 increasing glucose phosphorylation and insulin secretion, thereby improving glycemic
423 control [23, 25]. In a clinical trial, dorzagliatin directly increases insulin secretion and
424 glucose sensitivity in patients with GCK-MODY, suggesting that it may be able to
425 preserve GCK activity in GCK-MODY [26]. Our data further demonstrated that
426 dorzagliatin restored glucose threshold for insulin secretion and improved GSIS and
427 glucose intolerance in GCK-Q26L mutant mice (Fig, 5d-e). It is worthy to note that
428 dorzagliatin can increase insulin secretion in GCK-Q26L mice and decrease blood
429 glucose even in the fasting state with relatively low FBG in both WT and mutant mice
430 (Fig. 5a-c). However, there is no increased risk of hypoglycemia in a phase 3 clinical
431 trial dorzagliatin [23]. It remains to be determined whether this was caused by extra
432 high dose of dorzagliatin (about 15 times higher dose using in mice in this study than
433 recommend dose for patients with type 2 diabetes) or due to different responses of
434 different species.

435

436 In addition to dorzagliatin that directly targets to GCK, GLP-1RAs may also be

437 considered for the management of patients with GCK-MODY due to its beneficial
438 effect on glucose-dependent insulin secretion. Indeed, our data demonstrated that
439 liraglutide enhanced glucose sensing of mutant islets at physiological glucose
440 concentrations and improved GSIS (Fig. 6). Furthermore, a single administration of
441 liraglutide significantly decreased FBG in mutant mice without affecting FBG in WT
442 mice and markedly improved glucose tolerance (Fig, 6). These beneficial effects on
443 glucose sensing and insulin secretion, along with its role in promoting weight loss and
444 improving insulin resistance, make liraglutide (and possibly other GLP-1RAs) an
445 attractive option for managing GCK-MODY, particularly in patients with GCK-
446 MODY and insulin resistance.

447

448 To date, monogenic mutation involved in more than 70 genes have been identified to
449 cause monogenic diabetes. Some of the biggest challenges for early recognition and
450 diagnosis of monogenic diabetes are highly variable for disease penetrance and
451 clinical presentations in patients carrying different mutations in one gene or even the
452 same mutation in the same gene. Accumulating evidence indicates that genetic and/or
453 environmental factors may exacerbate or lessen the conditions, and many VUS can
454 have significant pathogenic effects when combined with other genetic predispositions
455 [4, 27]. In the current study, we found that the proband who carried a GCK-MODY
456 causing mutation inherited from her father, also possessed a high PRS for insulin

resistance that may have been inherited in part from her mother, whose PRS for insulin resistance was in top 1.09th percentile (Fig. 7). The elevated PRS may contribute to proband's atypical presentation including more severe hyperglycemia and dyslipidemia, supporting an additive effect that monogenic and polygenic factors may interact. These findings align with recent research indicating that PRS can substantially influence the clinical presentation of monogenic diseases, including diabetes [28, 29]. This dual influence underscores the complexity of diabetes pathogenesis and challenges the traditional dichotomy between monogenic and polygenic diabetes, highlighting the importance of considering polygenic factors even in cases initially attributed to single-gene mutations [30, 31]. Incorporating comprehensive genetic assessments, including PRS, into routine diabetes care could revolutionize how we predict, diagnose, and manage diabetes. Recognizing the role of PRS might help identify individuals at high risk for severe forms of diabetes, facilitating earlier interventions and more personalized management strategies [32]. Additionally, understanding the interplay between different genetic factors could lead to the development of targeted therapies that address specific mechanistic pathways involved in the disease [33, 34]. Recent studies have demonstrated the potential of such personalized approaches in improving disease prognosis [35].

Despite these promising findings, several limitations need to be acknowledged. First,

the study's reliance on a mouse model may not fully capture the complexity of human GCK-MODY and its interaction with insulin resistance. While the GCK-Q26L mutant mouse model provides valuable insights, human clinical trials are essential to validate the efficacy and safety of GKA and GLP-1RAs in GCK-MODY individuals with or without insulin resistance. Second, the study did not explore the long-term effects of these treatments on beta-cell function and overall metabolic health. Longitudinal studies are necessary to understand the potential benefits and risks associated with chronic use of these therapies. Third, the sample size and genetic diversity of the study population were limited. Future research should include larger, more diverse cohorts to ensure the generalizability of the findings. Furthermore, exploring gene-environment interactions will be crucial in elucidating the full impact of monogenic and polygenic factors on the development and progression of monogenic diabetes.

Author contributions

SJ, HS, and HZ designed and conducted experiments and analyzed data; SJ, HS, HZ YY, XL, SC, WF, JQ, JZ, and ZZ conducted experiments; All other authors revised the manuscript critically for important intellectual content. MW discussed project and edited manuscript; ML initiated and oversaw the project, designed the experiments, and wrote the manuscript.

Acknowledgments

The work was supported by the National Key R&D Program (2022YFE0131400 and 2019YFA0802502), and also by the National Natural Science Foundation of China (82220108014). We acknowledge the support of Tianjin Municipal Health Commission (TJWJ2021ZD001), Tianjin Medical University General Hospital Clinical Research Program (22ZYYLCZD02), Tianjin Municipal Science and Technology Commission (23JCQNJC00680 and 23JCQNJC00670), National Natural Science Foundation of China (82200892, 82301951, and 81800733), Tianjin Municipal Education Commission (2021KJ209), Tianjin Medical University Endocrine and Metabolic Disease the Youth Talent Incubator Program (2024XKNFM13), Tianjin Key Medical Discipline (Specialty) Construction Project (TJYXZDXK-030A), and Tianjin Medical University Clinical Special Disease Research Center - Neuroendocrine Tumor Clinical Special Disease Research Center.

Data availability

Due to local privacy laws and privileged human information, all requests for raw genotyping and clinical data are subject to prior approval from the local IRB. Analysis of the UK Biobank data was performed using application 89885. The UK Biobank data are available to researchers with research inquiries following IRB and UK Biobank approval (https://www.ukbiobank.ac.uk/enableyour-research/apply-for-access).The polygenic scores described in this publication are available for download from the Polygenic Score Catalog (https:// www.pgscatalog.org) under the publication ID PGP000223

Code availability

The manuscript described a pragmatic approach of publicly available software. Additional code is available upon request from the authors.

521 # References

522 [1] Matschinsky FM (1990) Glucokinase as glucose sensor and metabolic signal generator in
523 pancreatic beta-cells and hepatocytes. Diabetes 39(6): 647-652. 10.2337/diab.39.6.647

524 [2] Grimsby J, Sarabu R, Corbett WL, et al. (2003) Allosteric activators of glucokinase: potential
525 role in diabetes therapy. Science 301(5631): 370-373. 10.1126/science.1084073

526 [3] Matschinsky FM (2002) Regulation of pancreatic beta-cell glucokinase: from basics to
527 therapeutics. Diabetes 51 Suppl 3: S394-404. 10.2337/diabetes.51.2007.s394

528 [4] Stride A, Vaxillaire M, Tuomi T, et al. (2002) The genetic abnormality in the beta cell
529 determines the response to an oral glucose load. Diabetologia 45(3): 427-435. 10.1007/s00125-
530 001-0770-9

531 [5] Osbak KK, Colclough K, Saint-Martin C, et al. (2009) Update on mutations in glucokinase
532 (GCK), which cause maturity-onset diabetes of the young, permanent neonatal diabetes, and
533 hyperinsulinemic hypoglycemia. Hum Mutat 30(11): 1512-1526. 10.1002/humu.21110

534 [6] Steele AM, Shields BM, Wensley KJ, Colclough K, Ellard S, Hattersley AT (2014) Prevalence of
535 vascular complications among patients with glucokinase mutations and prolonged, mild
536 hyperglycemia. JAMA 311(3): 279-286. 10.1001/jama.2013.283980

537 [7] Chakera AJ, Steele AM, Gloyn AL, et al. (2015) Recognition and Management of Individuals
538 With Hyperglycemia Because of a Heterozygous Glucokinase Mutation. Diabetes Care 38(7):
539 1383-1392. 10.2337/dc14-2769

540 [8] Lotta LA, Gulati P, Day FR, et al. (2017) Integrative genomic analysis implicates limited
541 peripheral adipose storage capacity in the pathogenesis of human insulin resistance. Nat Genet
542 49(1): 17-26. 10.1038/ng.3714

543 [9] Oliveri A, Rebernick RJ, Kuppa A, et al. (2024) Comprehensive genetic study of the insulin
544 resistance marker TG:HDL-C in the UK Biobank. Nat Genet 56(2): 212-221. 10.1038/s41588-023-
545 01625-2

546 [10] Suzuki K, Hatzikotoulas K, Southam L, et al. (2024) Genetic drivers of heterogeneity in type 2
547 diabetes pathophysiology. Nature 627(8003): 347-357. 10.1038/s41586-024-07019-6

548 [11] Khera AV, Chaffin M, Aragam KG, et al. (2018) Genome-wide polygenic scores for common
549 diseases identify individuals with risk equivalent to monogenic mutations. Nat Genet 50(9):
550 1219-1224. 10.1038/s41588-018-0183-z

551 [12] Schroeder P, Mandla R, Huerta-Chagoya A, et al. (2023) Rare variant association analysis in
552 51,256 type 2 diabetes cases and 370,487 controls informs the spectrum of pathogenicity of
553 monogenic diabetes genes. medRxiv. 10.1101/2023.09.28.23296244

554 [13] Kingdom R, Beaumont RN, Wood AR, Weedon MN, Wright CF (2024) Genetic modifiers of

555 rare variants in monogenic developmental disorder loci. Nat Genet 56(5): 861-868.
556 10.1038/s41588-024-01710-0

557 [14] Fahed AC, Wang M, Homburger JR, et al. (2020) Polygenic background modifies penetrance
558 of monogenic variants for tier 1 genomic conditions. Nat Commun 11(1): 3635. 10.1038/s41467-
559 020-17374-3

560 [15] McCarthy MI (2017) Painting a new picture of personalised medicine for diabetes.
561 Diabetologia 60(5): 793-799. 10.1007/s00125-017-4210-x

562 [16] Iwani NA, Jalaludin MY, Zin RM, et al. (2017) Triglyceride to HDL-C Ratio is Associated with
563 Insulin Resistance in Overweight and Obese Children. Sci Rep 7: 40055. 10.1038/srep40055

564 [17] McLaughlin T, Abbasi F, Cheal K, Chu J, Lamendola C, Reaven G (2003) Use of metabolic
565 markers to identify overweight individuals who are insulin resistant. Ann Intern Med 139(10):
566 802-809. 10.7326/0003-4819-139-10-200311180-00007

567 [18] Pantoja-Torres B, Toro-Huamanchumo CJ, Urrunaga-Pastor D, et al. (2019) High
568 triglycerides to HDL-cholesterol ratio is associated with insulin resistance in normal-weight
569 healthy adults. Diabetes Metab Syndr 13(1): 382-388. 10.1016/j.dsx.2018.10.006

570 [19] Chiang JK, Lai NS, Chang JK, Koo M (2011) Predicting insulin resistance using the
571 triglyceride-to-high-density lipoprotein cholesterol ratio in Taiwanese adults. Cardiovasc
572 Diabetol 10: 93. 10.1186/1475-2840-10-93

573 [20] Das S, Forer L, Schonherr S, et al. (2016) Next-generation genotype imputation service and
574 methods. Nat Genet 48(10): 1284-1287. 10.1038/ng.3656

575 [21] Purcell S, Neale B, Todd-Brown K, et al. (2007) PLINK: a tool set for whole-genome
576 association and population-based linkage analyses. Am J Hum Genet 81(3): 559-575.
577 10.1086/519795

578 [22] Qiao J, Zhang Z, Ji S, et al. (2022) A distinct role of STING in regulating glucose homeostasis
579 through insulin sensitivity and insulin secretion. Proc Natl Acad Sci U S A 119(7).
580 10.1073/pnas.2101848119

581 [23] Zhu D, Li X, Ma J, et al. (2022) Dorzagliatin in drug-naive patients with type 2 diabetes: a
582 randomized, double-blind, placebo-controlled phase 3 trial. Nat Med 28(5): 965-973.
583 10.1038/s41591-022-01802-6

584 [24] Syed YY (2022) Dorzagliatin: First Approval. Drugs 82(18): 1745-1750. 10.1007/s40265-022-
585 01813-0

586 [25] Haddad D, Dsouza VS, Al-Mulla F, Al Madhoun A (2024) New-Generation Glucokinase
587 Activators: Potential Game-Changers in Type 2 Diabetes Treatment. Int J Mol Sci 25(1).
588 10.3390/ijms25010571

589 [26] Chow E, Wang K, Lim CKP, et al. (2023) Dorzagliatin, a Dual-Acting Glucokinase Activator,

590 Increases Insulin Secretion and Glucose Sensitivity in Glucokinase Maturity-Onset Diabetes of the
591 Young and Recent-Onset Type 2 Diabetes. Diabetes 72(2): 299-308. 10.2337/db22-0708

592 [27] Richards S, Aziz N, Bale S, et al. (2015) Standards and guidelines for the interpretation of
593 sequence variants: a joint consensus recommendation of the American College of Medical
594 Genetics and Genomics and the Association for Molecular Pathology. Genet Med 17(5): 405-424.
595 10.1038/gim.2015.30

596 [28] Khera AV, Chaffin M, Wade KH, et al. (2019) Polygenic Prediction of Weight and Obesity
597 Trajectories from Birth to Adulthood. Cell 177(3): 587-596 e589. 10.1016/j.cell.2019.03.028

598 [29] Johansson S, Irgens H, Chudasama KK, et al. (2012) Exome sequencing and genetic testing
599 for MODY. PLoS One 7(5): e38050. 10.1371/journal.pone.0038050

600 [30] Udler MS, McCarthy MI, Florez JC, Mahajan A (2019) Genetic Risk Scores for Diabetes
601 Diagnosis and Precision Medicine. Endocr Rev 40(6): 1500-1520. 10.1210/er.2019-00088

602 [31] Bonnefond A, Semple RK (2022) Achievements, prospects and challenges in precision care
603 for monogenic insulin-deficient and insulin-resistant diabetes. Diabetologia 65(11): 1782-1795.
604 10.1007/s00125-022-05720-7

605 [32] Pearson ER, Velho G, Clark P, et al. (2001) beta-cell genes and diabetes: quantitative and
606 qualitative differences in the pathophysiology of hepatic nuclear factor-1alpha and glucokinase
607 mutations. Diabetes 50 Suppl 1: S101-107. 10.2337/diabetes.50.2007.s101

608 [33] McCarthy MI (2010) Genomics, type 2 diabetes, and obesity. N Engl J Med 363(24): 2339-
609 2350. 10.1056/NEJMra0906948

610 [34] Le Collen L, Froguel P, Bonnefond A (2024) Towards the recognition of oligogenic forms of
611 type 2 diabetes. Trends Endocrinol Metab. 10.1016/j.tem.2024.06.006

612 [35] Inshaw JRJ, Cutler AJ, Crouch DJM, Wicker LS, Todd JA (2020) Genetic Variants Predisposing
613 Most Strongly to Type 1 Diabetes Diagnosed Under Age 7 Years Lie Near Candidate Genes That
614 Function in the Immune System and in Pancreatic beta-Cells. Diabetes Care 43(1): 169-177.
615 10.2337/dc19-0803

616

617

618

619

a

Time (mins)	Glucose (mmol/L)	Insulin (mIU/L)	C-Peptide (ng/mL)
0	6.29	14.80	1.37
30	11.93	21.60	2.22
60	17.20	30.50	3.32
120	18.04	34.60	4.73
180	14.46	29.70	4.89

c

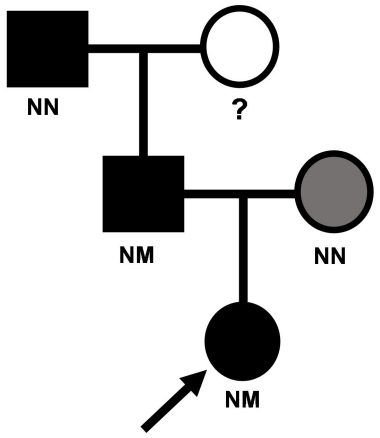

b

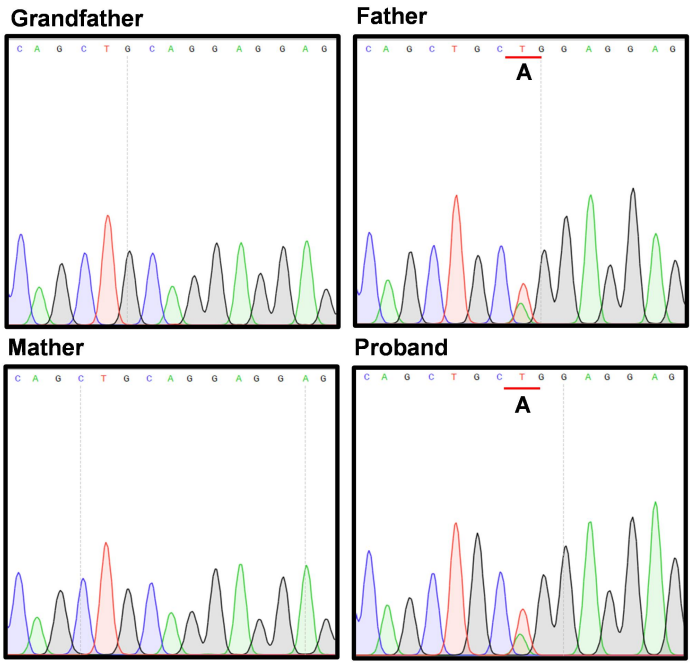

Figure 1. Proband with impaired insulin secretion and diabetes carries a GCK missense mutation (c.77A>T, p.Q26L) that was inherited from her father. (**a**) The results of blood glucose, insulin, and C-Peptide of the proband during OGTT performed at the onset of diabetes. (**b**) A missense mutation in GCK gene (c.77A>T, p.Q26L) was identified in the proband and her father by WES confirmed by Sanger sequencing. (**c**) Pedigree analyses showed that GCK-Q26L was inherited from proband's father. Squares represent males and circles represent females. Filled black symbols indicated members affected with diabetes, gray symbol represented the member with the pre-diabetes. The proband was indicated with a black arrow. Where tested, the genotypes of family members were given (N, normal allele; M, mutant allele; NN, normal genotype; NM,

11 heterozygous genotype).

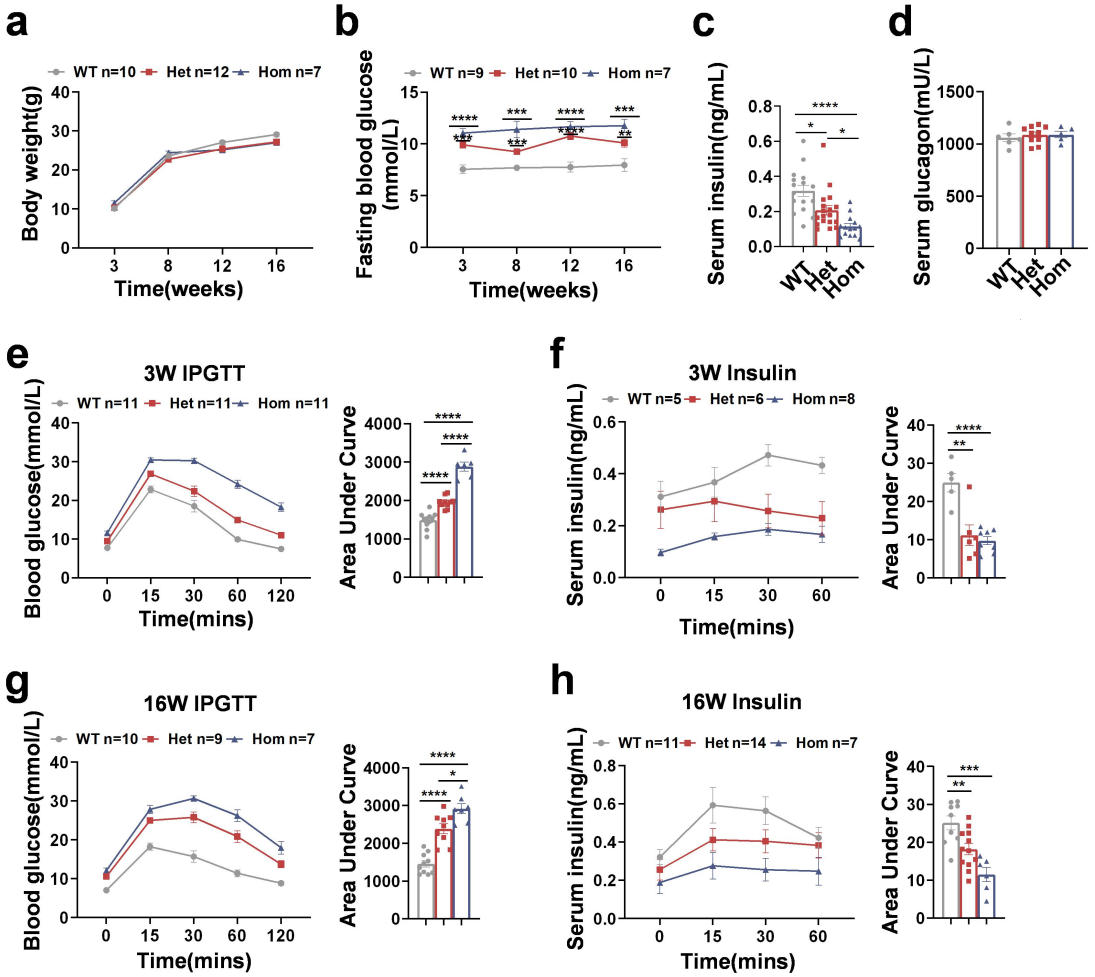

Figure 2. GCK-Q26L causes glucose intolerance in a dose-dependent manner. (**a**, **b**) Body weight (**a**) and fasting blood glucose (**b**) of male mice were measured at 3, 8, 12, 16 weeks of age. WT *vs* Het, WT *vs* Hom, ** P < 0.01, *** P < 0.001, **** P < 0.0001. (**c**) Fasting serum insulin in three-group 16-week-old male mice were measured by ELISA. (**d**) Fasting serum glucagon in three-group 16-week-old male mice were measured by ELISA. (**e**) IPGTT in 3-week-old male mice (2 g/kg i.p.) and the area under curve (AUC) of blood glucose during IPGTT. (**f**) Serum insulin levels in 3-week-old male mice during IPGTT were measured by ELISA, with calculated AUCs. (**g**) IPGTT in 16-week-old male mice (2 g/kg i.p) and the AUC of blood glucose. (**h**) Serum insulin levels in 16-week-old male mice during IPGTT were measured by ELISA, with calculated AUCs. Each data point represents an individual mouse. Values are shown as mean ± SEM. WT *vs* Het, WT *vs* Hom, Het *vs* Hom, *P < 0.05, **** P < 0.0001.

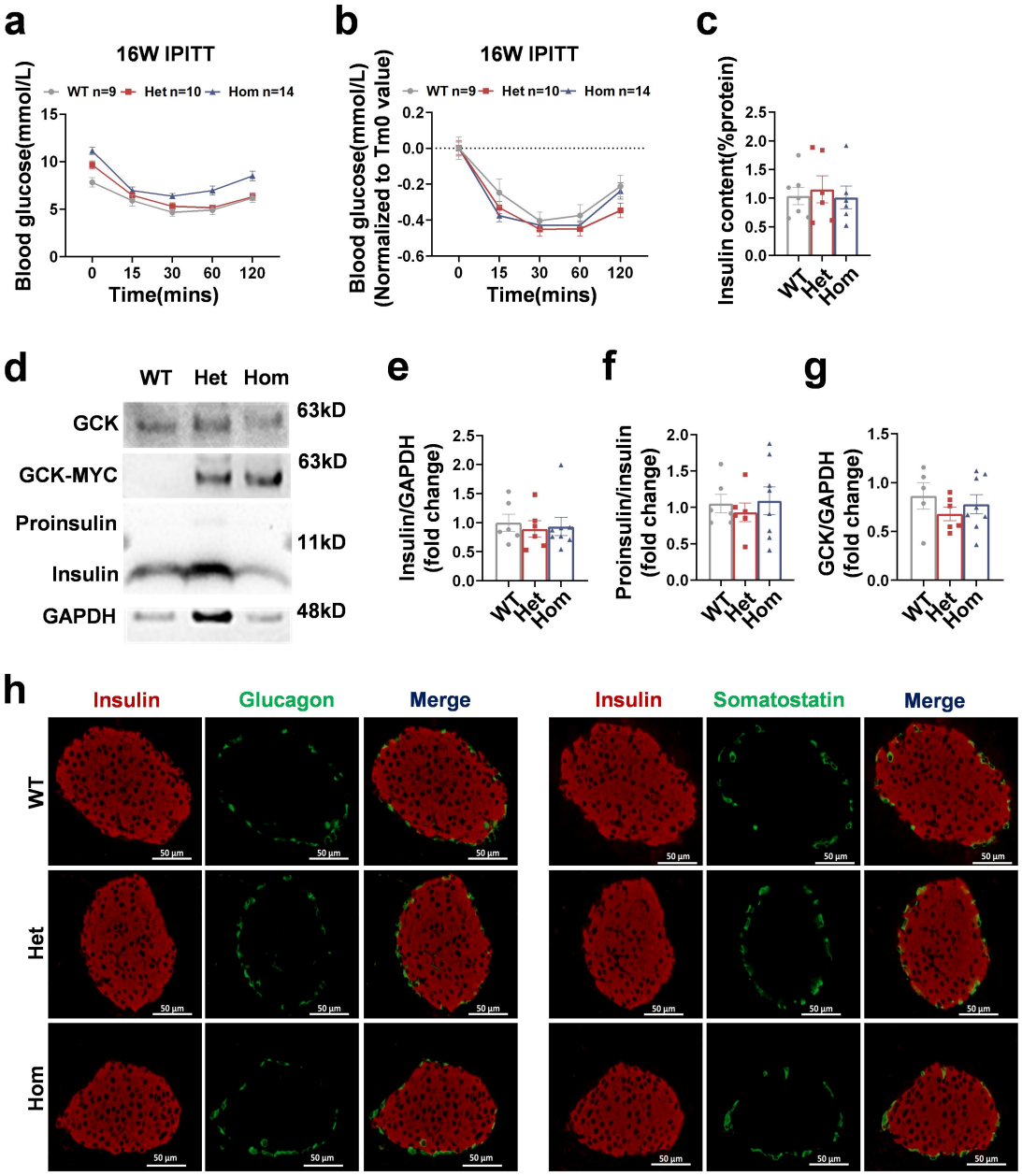

Figure 3. GCK-Q26L did not affect insulin sensitivity, insulin content, and islet cell composition. (**a, b**) IPITT were performed in 16-week-old male mice (0.7 U/kg i.p), (**b**) was (**a**) normalized to the baseline of blood glucose. (**c**) Islet insulin content of 16-week-old male mice was measured by ELISA**.** (**d**) Islets isolated from 10-week-old male mice were directly lysed. Western blots were performed to detect endogenous GCK, MYC-tagged GCK (GCK-MYC), proinsulin and insulin as indicated. GAPDH was used as a loading control. Quantification of insulin (**e**), the ratio of proinsulin to insulin (**f**), and GCK (**g**)**.** (**h**) Representative immunofluorescence images of anti-insulin (red), anti-glucagon (green) and

anti-somatostatin(green) antibodies in pancreatic sections from 12-week-old male mice. Scale bar = 50 μm (n = 3 mice/group). Each data point represents an individual mouse. Values were shown as mean ± SEM.

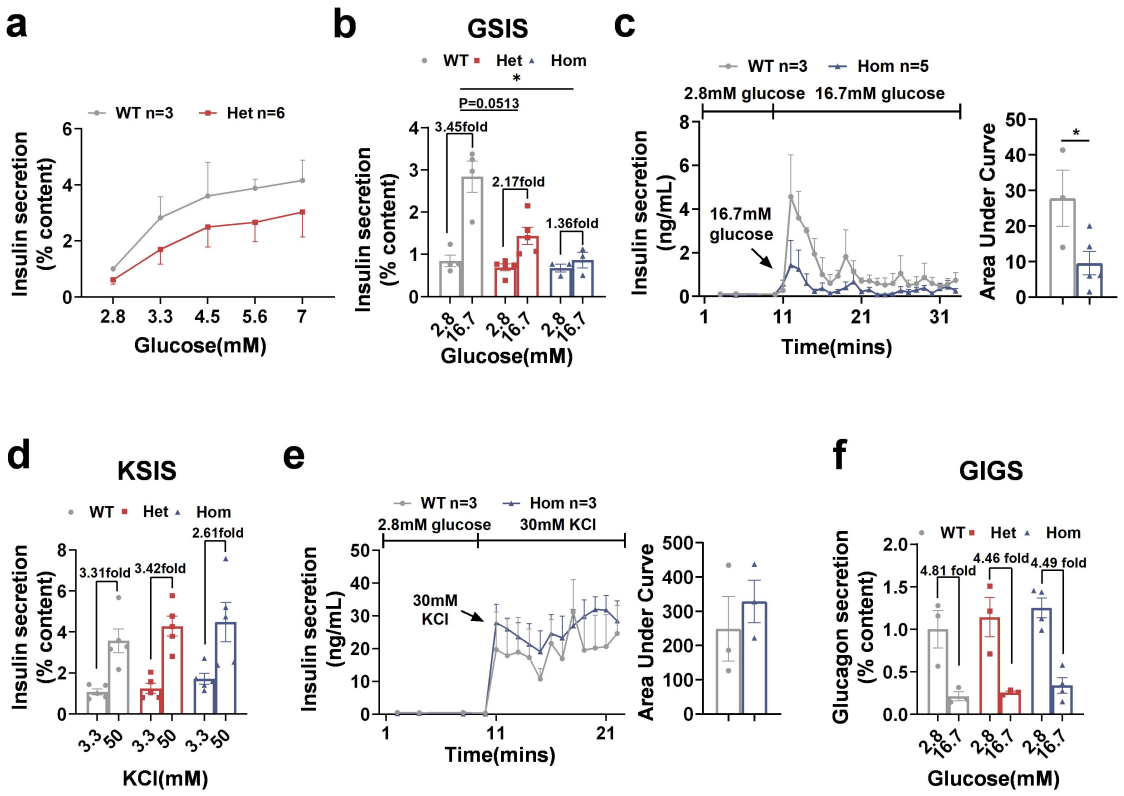

Figure 4. GCK-Q26L impaired glucose-stimulated insulin secretion without affecting potassium-stimulated insulin secretion and glucose-inhibited glucagon secretion. (**a**) Dose-dependent effects of glucose on insulin secretion of 16-week-old male WT and Het mice. Isolated islets successively incubated in 2.8, 3.3, 4.5, 5.6 and 7 mmol/L glucose. (**b**) Islets isolated from 10-week-old male WT, Het and Hom mice were incubated with 2.8 mmol/L for 1 hour followed by stimulated with either low (2.8 mmol/L) or high (16.7 mmol/L) glucose for 2 hours. Insulin secretion response to low and high glucose were measured. (**c, e**) Dynamic insulin secretion of 10-week-old male WT and Hom mice islets cultured in the perfusion chamber with continues buffer renewal (2.8 mmol/L glucose, 16.7 mmol/L glucose, 2.8 mmol/L glucose, 30 mmol/L potassium), with calculated AUCs. (**d**) Islets isolated from 10-week-old male WT, Het and Hom mice were incubated with 2.8 mmol/L glucose for 1 hour followed by stimulated with either low (3.3 mmol/L) or high (50 mmol/L) potassium for 2 hours. Insulin secretion response to low and high potassium were measured. (**f**) Glucagon secretion measured in isolated islets from 10-week-old male WT, Het and Hom mice when incubated in 2.8 and 16.7 mmol/L glucose. Each data point represents an individual mouse. Values are shown as mean ± SEM. * $P < 0.05$.

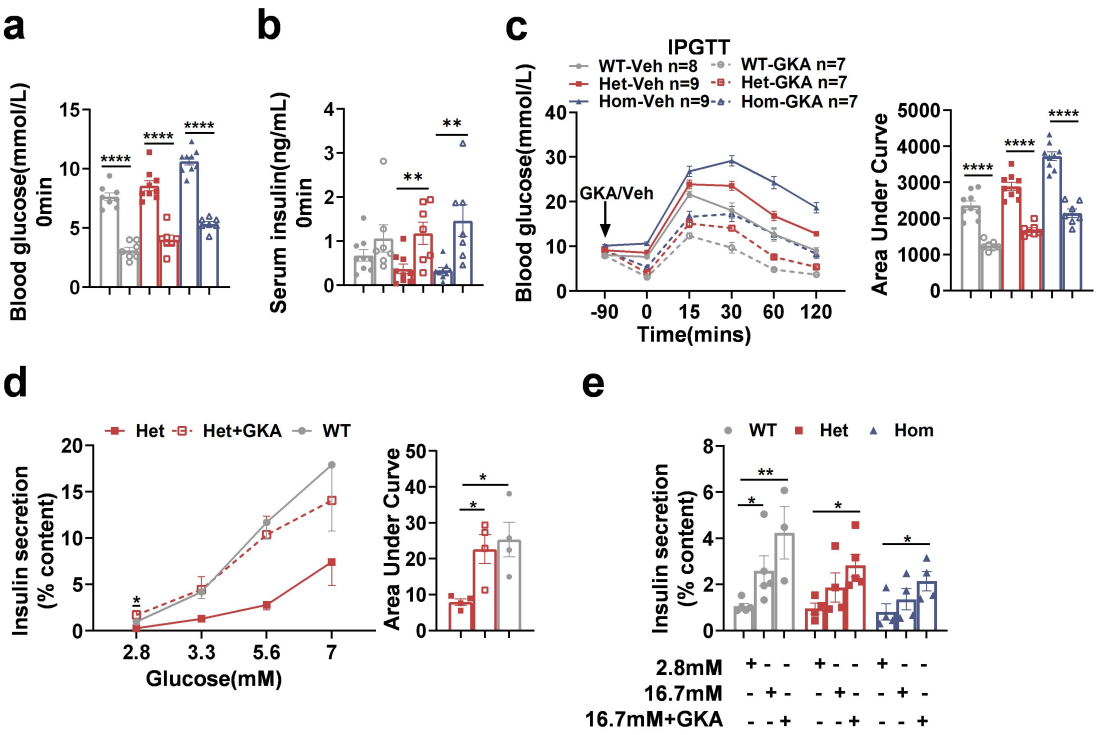

Figure 5. Dorzagliatin (GKA) restores the glucose threshold for insulin secretion and ameliorates glucose tolerance in GCK-Q26L mice. (**a-c**) We performed IPGTT on 10-week-old male mice (2 g/kg i.p), and vehicle (0.9% Nacl) or GKA (30 mg/kg) was administered orally to mice 90 minutes before glucose challenge. Blood glucose (**a**) and serum insulin level (**b**) before glucose challenge. (**c**) Blood glucose and AUC of IPGTT. (**d**) Dose-dependent effects of glucose on insulin secretion of 10-week-old male WT and Het mice with or without 30 uM GKA, and the AUC of Insulin secretion. Het *vs* Het-GKA, *P < 0.05. (**e**) Insulin secretion measured in isolated islets from 10-week-old male WT, Het and Hom mice when incubated in 2.8, 16.7 mmol/L glucose and 16.7 mmol/L glucose containing 30 uM GKA. Each data point represents an individual mouse. Values are shown as mean ± SEM. * P < 0.05, ** P < 0.01, **** P < 0.0001.

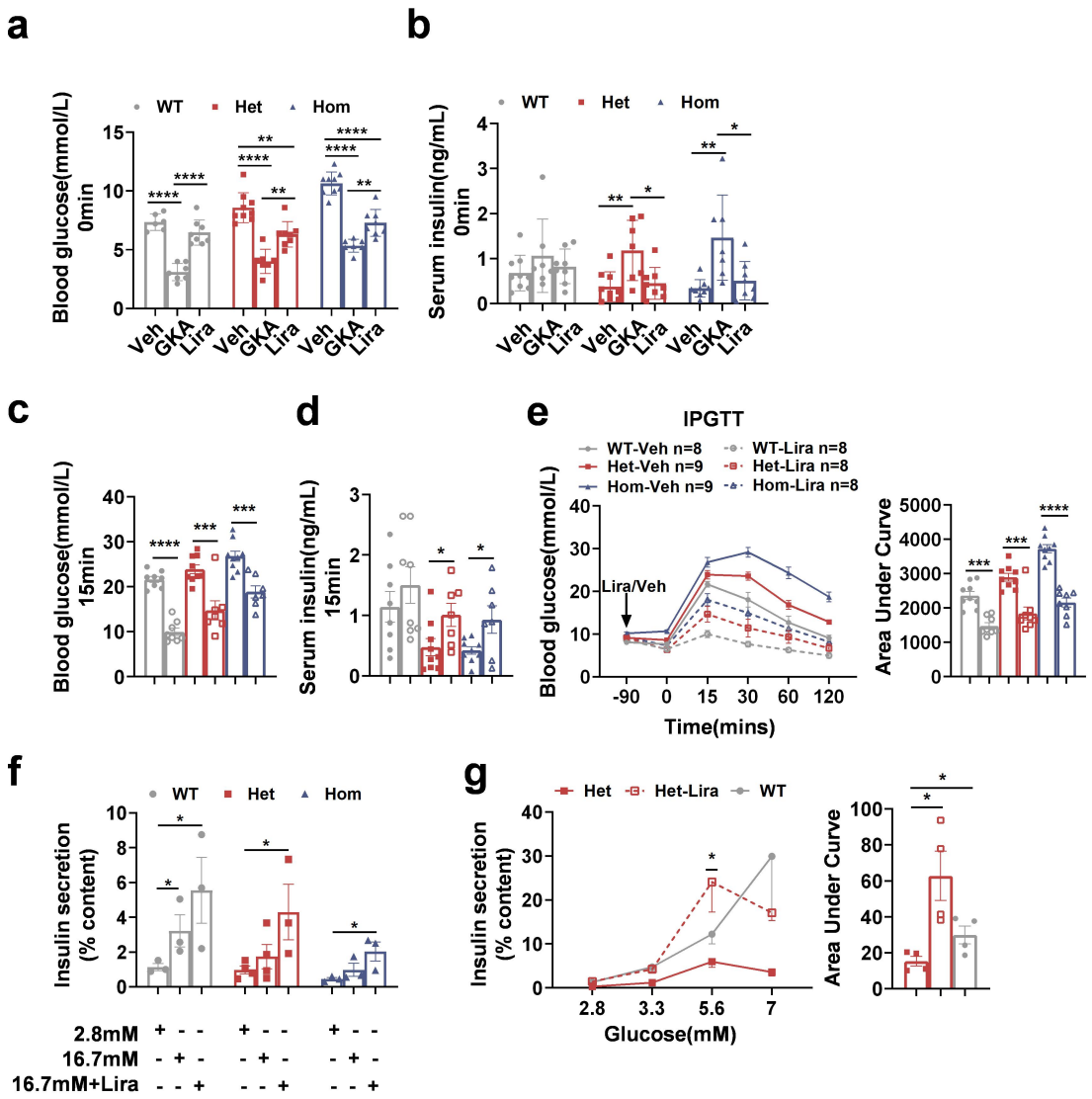

Figure 6. Liraglutide amplifies insulin secretion response to glucose and ameliorates glucose tolerance in GCK-Q26L mice. (**a, b**) For liraglutide, we conducted experiments similar to those shown in Figure 5 with dorzagliatin, assessing blood glucose (**a**) and serum insulin levels (**b**) in mice that had been treated with dorzagliatin and liraglutide prior to glucose challenge. (**c-e**) show the results of IPGTT with Liraglutide. Blood glucose (**c**) and serum insulin level (**d**) 15 minutes after glucose challenge. (**e**) IPGTT and the AUC of blood glucose. (**f**) Insulin secretion measured in isolated islets from 10-week-old male WT, Het and Hom mice when incubated in 2.8, 16.7 mmol/L glucose and 16.7 mmol/L glucose containing 100 nM Lira. (**g**) Dose-dependent effects of glucose on insulin secretion and the AUC of 10-week-old male WT and Het mice with or without 100 nM Lira, Het *vs* Het-Lira, * $P < 0.05$. Each data point represents an individual mouse. Values are shown as mean ± SEM. * $P < 0.05$ *** $P < 0.001$, **** $P < 0.0001$.

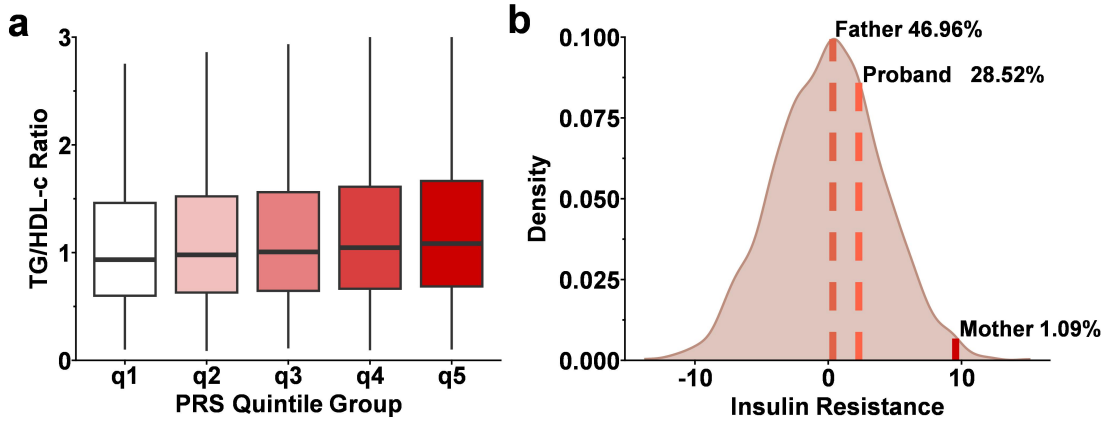

Figure 7. Quality control and PRS score for study samples. (**a**) The distribution of the ratio of triglycerides to HDL cholesterol as a function of quintiles of an insulin resistance (IR) polygenic risk score (PRS) was evaluated in 424,664 UK Biobank samples. The horizontal line in the box indicates the median value, and the top and bottom of the box indicate the upper and lower quartiles, respectively. (**b**) The results of insulin resistance polygenic risk score analysis on case family. The curve denotes the probability density function of the IR PRS scores from the 1000 Genomes Project East Asian samples. Vertical dashed lines indicate the PRS for each family member: the father's position at the top 46.96th percentile, the proband at the top 28.52th percentile, and the mother at the top 1.09th percentile.

Table 1. Clinical features of the family of the proband carrying GCK(Q26L) mutation

	Proband	Father	Mother
Age at diagnosis	Teens	Thirties	/
Gender	Female	Male	Female
BMI at present (kg/m^2)	26.76	25.54	29.78
Clinical symptoms at onset	Polydipsia, polyuria, polyphagia, weight loss and ketosis	found elevated FBG in a physical examination	/
FBG at diagnosis (mmol/L)	6-7	5-7	/
FBG at present (mmol/L)	7.5-13.2	6.5	6.4
HbA1c at diagnosis (mmol/mol)	113.12 (12.5%)	/	/
HbA1c at present (mmol/mol)	132.79 (14.3%)	60.66 (7.7%)	44.26 (6.2%)
Total cholesterol (mmol/L)	5.85	5.44	4.19
Triglycerides (mmol/L)	10.39	0.80	1.11
HDL-cholesterol (mmol/L)	0.74	1.03	0.78
LDL-cholesterol (mmol/L)	3.88	3.90	3.24
Islet autoantibodies	Negative	/	/
Treatment at diagnosis	Metformin 0.5g TID	Metformin 0.5g BID	/

	Insulin glargine：18U QN	Vildagliptin 50mg BID	
Treatment at present	Metformin 0.5g TID Insulin aspart：8-6-6U Insulin glargine：12U QN	Metformin 0.5g BID	/
Complications and comorbidities	No	Diabetic retinopathy (non-proliferative stage)	/

Note: BMI, body mass index; FBG, fasting blood glucose; HDL, high density lipoprotein; LDL, low density lipoprotein; OGTT, oral glucose tolerance test; OHA, oral hypoglycemic agent; Islet autoantibodies, GADA(glutamate decarboxylase antibody)、ICA(islet cell antibody)、 IA-2A(protein tyrosine phosphatase-like protein antigen)、 ZnT8A(Zinc transporter 8 antibody)；TID, ter in die; BID, bis in die; QN, quāque nocte; “/”, none or not provided.